between two copper ions with no intervening oxide ions (along the *z* axis) is minimized by the presence of a pair of electrons in the d_{z^2} orbitals. It has occurred to us that the coulomb repulsion energy in a chain of Cu^{2+} ions may be reduced to three-fourths if there is a disproportionation leading to an alternation of Cu^+ and Cu^{3+} ions along the chain such as $Cu_1{}^{1+}$–$Cu_2{}^{3+}$–$Cu_3{}^{1+}$–$Cu_4{}^{3+}$···. For an isolated antiferromagnetically coupled ($S = 0$) $Cu_A{}^{2+}$–$Cu_B{}^{2+}$ dimer, such a disproportionation can lead to two additional singlet states, $Cu_A{}^{+}$–$Cu_B{}^{3+}$ and $Cu_A{}^{3+}$–$Cu_B{}^{+}$, assuming that the Cu^{3+} ion is in the low-spin state. These additional singlet states will be degenerate in the case of isolated dimers with equivalent copper sites. In a linear chain, however, the disproportionation may stabilize a charge density wave (CDW) in which there is an alternation of Cu^+ and Cu^{3+}. Such a CDW would be further stabilized if there are two inequivalent copper sites favoring Cu^+ and Cu^{3+} as is likely in the *I*4 symmetry of Bi_2CuO_4. The degeneracy of the two disproportionated states in the dimers would then be lifted, and one singlet state may become more stabilized compared to the other. The good fit to the susceptibility of Bi_2CuO_4 found with the factor of $^2/_3$ in the denominator in eq 2 instead of the factor of $^1/_3$ used in the classical Bleaney–Bowers expression suggests that one of the singlet states is much more stabilized compared to the other.[53] Such a disproportionation may be important for the unscreened $-Cu_I-Cu_I-Cu_I-$ chains along the *a* axis of $YBa_2Cu_3O_7$.

Concluding Remarks

In this article we have studied a large number of ternary copper oxide systems having structural features common to the two known families of the high-temperature superconducting phases. The main conclusions that can be derived from these studies are as follows: (i) The magnitude and temperature dependence of the magnetic susceptibility are dependent more on the geometry of the extended copper–oxygen framework rather than the local geometry around the Cu^{2+} ion. (ii) While compounds with extended 180° Cu–O–Cu interactions show high antiferomagnetic interaction strength and low, nearly temperature-independent susceptibility, no ferromagnetic interaction was observed in compounds with 90° Cu–O–Cu superexchange interaction. (iii) Compounds in which Cu^{2+} ions are isolated with competing superexchange interactions show high temperature-dependent susceptibility. (iv) The Cu–O–O–Cu interaction (found between the planes of the oxide superconductors) is relatively weak compared with the Cu–O–Cu superexchange interaction. However, the antiferromagnetic coupling temperatures are close to the superconducting temperatures. The possibility of a disproportionation of Cu^{2+} to Cu^+ and Cu^{3+} has been considered for the reduction of the magnetic moment observed in compounds such as Bi_2CuO_4 in which there exists direct Cu–Cu interaction. A puzzling result is that in the $La_2Ni_{1-x}Cu_xO_4$ system there is no contribution to the susceptibility from the Cu^{2+} ions even for small values of *x*.

Acknowledgment. We thank Professor C. N. R. Rao for encouragement and the University Grants Commission, New Delhi, India, for financial support.

Registry No. Ca_2CuO_3, 12213-78-4; Sr_2CuO_3, 12443-63-9; $Sr_2CuO_2Cl_2$, 57363-72-1; $Ba_2Cu_3O_4Cl_2$, 58206-72-7; Bi_2CuO_4, 39368-32-6; $La_{1.8}Ba_{1.2}Cu_{0.9}O_{4.8}$, 57608-96-5; $MgCu_2O_3$, 57608-96-5; $BaCuO_2$, 57348-58-0; $Y_2Cu_2O_5$, 12158-85-9; Li_2CuO_2, 12527-46-7; CuO, 1317-38-0; $CaCO_3$, 471-34-1; $Sr(NO_3)_2$, 10042-76-9; $SrCO_3$, 1633-05-2; $SrCl_2$, 10476-85-4; $BaCO_3$, 513-77-9; $BaCl_2$, 10361-37-2; Bi_2O_3, 1304-76-3; La_2O_3, 1312-81-8; $Ba(NO_3)_2$, 10022-31-8; $MgCO_3$, 546-93-0; Y_2O_3, 1314-36-9; LiOH, 1310-65-2; $Cu(NO_3)_2$, 3251-23-8.

---

(53) Sreedhar, K.; Ganguly, P.; Ramasesha, S. *J. Phys. C* **1988**, *21*, 1129.

Contribution from the Department of Chemistry,
University of Alberta, Edmonton, Alberta, Canada T6G 2G2

Synthesis and Structure of a Diphosphetene, $(CF_3)\overline{P(CF_3)PC(SiMe_3){=}C}(SiMe_3)$, and the Coordination and Metallacycle Formation of Several Diphosphetenes with Iridium(I)

Ian G. Phillips, Richard G. Ball, and Ronald G. Cavell*

Received September 25, 1987

New diphosphetenes $(CF_3)\overline{P(CF_3)PC(R){=}C}(R')$, **9** (R = R′ = SiMe₃), **10** (R = R′ = Ph), and **11** (R = CH_3, R′ = $SiMe_3$), have been prepared by the reaction of $(CF_3P)_{4,5}$ and the appropriate alkyne. The first of these has been structurally characterized. For **9** at −65 °C (monoclinic *C*2/*c*, No. 15): $a = 17.057$ Å, $b = 8.811$ Å, $c = 11.983$ Å, $\beta = 102.13°$, and $Z = 4$. The central P_2C_2 ring is slightly twisted from planarity (the angle between the PP vector and the CC vector is 12.8°). Major bond lengths are P–P = 2.223 (1) Å, $P–C_{endo}$ = 1.841 (2) Å, and C–C = 1.356 (3) Å. The new diphosphetenes **10** and **11** and also $(CF_3)\overline{P(CF_3)PC(CF_3){=}C}(CF_3)$ (**1**) (prepared in 1964 by W. Mahler) react with *trans*-$[IrCl(N_2)(PPh_3)_2]$ at low temperature to form an η^1 (phosphorus) complex, which transforms to a metallacycle with the

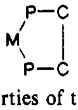

framework at ordinary temperatures. NMR spectral properties of the diphosphetenes, the η^1 complexes, and the metallacycles are given.

Introduction

In 1964 Mahler[1] reported the synthesis and characterization of the first 1,2-diphosphetene (**1**) and the 1,2,3-triphospholene (**2**) by copyrolysis of $[CF_3P]_{4,5}$ with excess hexafluorobut-2-yne at 170 °C (eq 1, R = R′ = CF_3, 170 °C, 3 days). Heating $[(CF_3)P]_{4,5}$ with $CH_3C{\equiv}CCH_3$ under similar conditions produced a triphospholene $(CF_3)\overline{P(CF_3)P(CF_3)PC(CH_3){=}C}(CH_3)$ (**3**), which was characterized by its NMR spectra, but no corresponding diphosphetene was obtained.[2] Reinvestigation of the pyrolysis of $[PhP]_5$ with $PhC{\equiv}CPh$ (a reaction first reported by Ecker and Schmidt[3] in 1973) by Mathey et al.[4,5] showed that the scope of this preparative route could be broadened. Improved yields and alternative synthesis of other diphosphetenes and tri-

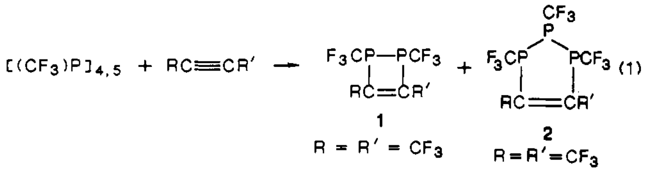

---

(1) Mahler, W. *J. Am. Chem. Soc.* **1964**, *86*, 2306.

(2) Mahler, W., personal communication 1986.

(3) Ecker, A.; Schmidt, U. *Chem. Ber.* **1973**, *106*, 1453.

(4) Charrier, C.; Guilhem, J.; Mathey, F. *J. Org. Chem.* **1981**, *46*, 3.

(5) Charrier, C.; Margiot, N.; Mathey, F.; Robert, F.; Jeannin, Y. *Organometallics* **1986**, *5*, 623.

0020-1669/88/1327-2269$01.50/0

phospholenes (via lithiation of heterocycles prepared by the pyrolysis route) and the complete structural refinement of two diphosphetenes (Ph)P(Ph)PC(R)=C(R) (R = Ph (**4**); R = *t*-Bu (**5**)) have been reported.[4,5]

Other synthetic routes to unsaturated polyphosphane heterocycles (yielding exclusively 1,2-diphosphetenes) are the photocleavage of a *P*-phenylphosphaalkene in the presence of PhC≡CPh,[6] the [2 + 2] head to head dimerization of a phosphaalkene,[7] and cyclization of 1,4-diphosphabutadienes.[8]

As part of our studies of the coordination chemistry of perfluoromethyl homo- and heterocyclopolyphosphanes[9] we have used the pyrolysis of $[(CF_3)P]_{4,5}$ with a variety of substituted acetylenes to obtain ligands with a variety of backbone substituents.

The coordination chemistry of these ligand systems is generally unexplored. A brief report of the coordination chemistry of **1** with iron carbonyls demonstrated η^1-phosphorus lone-pair coordination to give **6** (eq 2).[10] An analogous study[4] yielded evidence for a

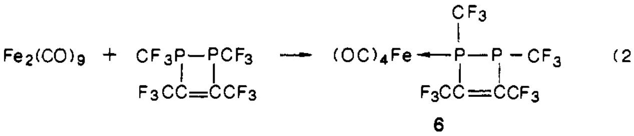

6 (2)

related unstable complex of **4** characterized only by its infrared spectrum. Also reported was a $[Fe_2(CO)_6]$ derivative **7**, which on heating lost a tolane subunit to give, as the major product, a previously described phosphinidene complex **8**.[4]

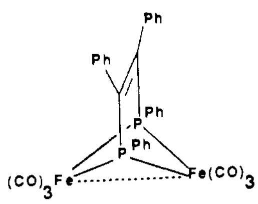

7

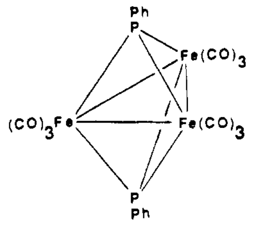

8

Experimental Section

All materials were manipulated by using standard vacuum-line or Schlenk techniques (Ar).[11] Pyrolyses were carried out in sealed glass tubes. The $[(CF_3)P]_{4,5}$ mixture[12] was prepared by mercury reduction of CF_3PI_2.[13] Commercial supplies of the acetylenes (Aldrich, Petrarch) were used without further purification. Compound **1**[1] and the transition-metal substrate[14] *trans*-$[IrCl(N_2)(PPh_3)_2]$ were prepared according to the literature procedures.

NMR spectra were recorded on a Bruker WP-400 (^{31}P (162 MHz) and ^{19}F (376.5 MHz)) or a AM-300 (^{1}H and ^{13}C (75.5 MHz)) instrument. Pyrolysis reactions were monitored by ^{19}F and ^{1}H NMR spectra of the neat reaction mixtures recorded at room temperature on a Bruker WP-80 spectrometer. Mass spectra were recorded on a Kratos MS50 instrument. Microanalyses were performed in this department.

Preparation of $(CF_3)P(CF_3)PC(SiMe_3)=C(SiMe_3)$ (9). $[(CF_3)P]_{4,5}$ (1.86 g, 9.3 mmol as "$(CF_3P)_2$") and $Me_3SiC≡CSiMe_3$ (1.54 g, 9.1 mmole) were heated to 180 °C for 110 h in a sealed 10-mL glass reaction tube equipped with a breakseal. The volatile products of the reaction were dynamically fractionated through traps maintained at 0, −78 and −196 °C on a vacuum (10^{-4} Torr) manifold as the reaction product mixture was warmed to 150 °C. Masses of colorless crystalline solids contaminated with a yellow oil were obtained in the 0 °C fraction. The −78 °C fraction contained $[(CF_3)P]_{4,5}$ (50% of the material taken was recovered unreacted) and unseparated product diphosphetene, while Me_3SiF was the principal component of the −196 °C fraction.

Table I. Heterocyclopolyphosphanes Obtained from (Trifluoromethyl)(cyclo)polyphosphanes and Acetylenes

		rel yield		
	% yield[a]	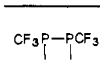	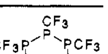	ref
R = R′ = CF_3		0.55 (**1**)	0.35 (**2**)	1
R = R′ = CH_3			1.00 (**3**)	2
R = R′ = $Si(CH_3)_3$	13	0.95 (**9**)	0.05	*b*
R = R′ = C_6H_5	27	0.85 (**10**)	0.15	*b*
R = CH_3, R′ = $Si(CH_3)_3$	10	0.80 (**11**)	0.20	*b*

[a] Of the diphosphetene as isolated. [b] This work.

Sublimation of the 0 °C fraction in a water-cooled cold finger apparatus (+25 °C, 10^{-3} Torr) for 40 h gave 0.448 g of **9** as colorless crystals: mp 68.5–69.0 °C; yield 13%. Mass spectral data, *m/e*: 370, $[M]^+$ (100, reference); 209, $[M - CF_4, Me_3Si]^+$ (21); 186, $[M - 2Me_3SiF]^+$ (81); 73, $[Me_3Si]^+$ (75). Anal. Calcd for $C_{10}H_{18}P_2Si_2$: C, 32.43; H, 4.89. Found: C, 32.26; H, 4.90. ^{13}C NMR data: −0.84 ppm, singlet [$^1J_{C,Si}$ = 52.7 Hz, $(CH_3)_3Si$]; +129.96 ppm, doublet of quartets [$^1J_{C,F}$ = 324.0 Hz, $^1J_{C,P}$ = 68.0 Hz, CF_3P]; +176.47 ppm, doublet [$^1J_{C,P}$ = 23.4 Hz, =*C*P]. Crystals of **9** suitable for X-ray crystallography were obtained by sublimation in a 50 × 1 cm sealed glass tube half immersed in water at a temperature of 40 °C for 20 h. Preparation yields are summarized in Table I.

Preparation of $(CF_3)P(CF_3)PC(Ph)=C(Ph)$ (10). As for **9**, $[(CF_3)P]_{4,5}$ (1.10 g, 5.5 mmol as "$(CF_3P)_2$") and PhC≡CPh (0.90 g, 5.0 mmol) were heated to 180 °C for 72 h. The 0 °C fraction (1.42 g) contained $(CF_3)P(CF_3)PC(Ph)=C(Ph)$ and $(CF_3)P(CF_3)P(CF_3)PC(Ph)=C(Ph)$ as an 85:15 mixture. Room-temperature sublimation in a cold finger apparatus gave pure **10** (0.47 g) in the last two of five fractions obtained over 40 h: yield 27%, mp 112–113 °C. Mass spectral data, *m/e*: 378, $[M]^+$ (100, reference; 309, $[M - CF_3]^+$ (48); 259, $[M - C_2F_5]^+$ (75); 240, $[M - C_2F_6]^+$ (35); 209, $[M - P(CF_3)_2]^+$ (33); 178, $[Ph_2C_2]^+$ (26). Anal. Calcd for $C_{16}H_{10}F_6P_2$: C, 50.81; H, 2.67. Found: C, 50.64; H, 2.65. ^{13}C NMR data: +129.27 ppm, quartet of doublets [$^1J_{C,F}$ = 324.0 Hz, $^1J_{C,P}$ = 60.4 Hz, *C*F_3P]; +143.34 ppm, multiplet [=*C*P]; +134.50 ppm, pseudotriplet X of AA′X [$|^2J_{C,P} + {}^3J_{C,P}|$ = 15.1 Hz, ipso-C of Ph]; +127.55, triplet (br) X of AA′X [$|^3J_{C,P} + {}^4J_{C,P}|$ = 6 Hz, *o*-C of phenyl]; +129.96 and −128.97 ppm, singlets [*m*- and *p*-C of Ph].

Preparation of $(CF_3)P(CF_3)PC(CH_3)=CSi(CH_3)_3$ (11). $[(CF_3)P]_{4,5}$ (0.71 g, 3.6 mmol as "$(CF_3P)_2$") and MeC≡CSiMe₃ (0.40 g, 3.6 mmol) were heated to 180 °C for 24 h. Fractional distillation of the volatile products through traps maintained at −23, −45, −78, and −196 °C gave three fractions. The approximately 800 mg of colorless liquid trapped at −23 °C comprised **11** and the related triphospholene **11b** as an 80:20 mixture. The −45 °C fraction was pure **11** by ^{31}P, ^{19}F, ^{13}C, and ^{1}H NMR spectroscopy: estimated mass ca. 100 mg, yield ~10%. Mass spectral data, m/e: 312, $[M^+]$ (82); 170, $[M - CF_3, SiMe_3]^+$ (35); 151, $[M - CF_4, SiMe_3]^+$ (99); 101, $[M - 2CF_3, SiMe_3]^+$ (23.4); 89, $[C_4H_3F_2]^+$ (21.0); $[C_3H_3F_2]^+$ (32); 73, $[Me_3Si]^+$ (100, reference). ^{13}C NMR data: −1.35 ppm, singlet [$^1J_{C,Si}$ = 52.1 Hz, $(CH_3)_3Si$]; +24.90 ppm, doublet of doublets [$^2J_{C,P}$ = 17.4 Hz, $^3J_{C,P}$ = 4.5 Hz, *C*H_3C=]; +130.20 ppm, quartet of doublets [$^1J_{C,F}$ = 332.6 Hz, $^1J_{C,P}$ = 69.8 Hz, (*C*F_3)P]; +129.83 ppm, quartet of doublets [$^1J_{C,F}$ = 323.0 Hz, $^1J_{C,P}$ = 63.8 Hz, (*C*F_3)P]; +160.76 ppm, pseudotriplet X of ABX [$|^1J_{C,P} + {}^2J_{C,P'}|$ = 10.0 Hz, =*C*P]; +156.23 ppm, singlet [=*C*P]. The −78 °C fraction contained $CH_3C≡CSiMe_3$, traces of **11**, and unknowns, of mass <100 mg. A dark brown residue remained in the reaction vessel, and no material was collected in the −196 °C trap.

Preparations of 12–16. Typically $[IrCl(N_2)(PPh_3)_2]$ (0.05 mmol), a diphosphetene (**1**, **9**, **10**, **11**; 0.05–1.00 mmol) and $CDCl_3$ (ca. 400 μL) were sealed in 5-mm NMR tubes at −196 °C. The frozen samples were warmed to −78 °C for 5 min and then to −50 °C for 1–2 min whereupon reaction ensued as evidenced by the evolution of N_2. The samples remained unchanged indefinitely when stored at −78 °C in an acetone/dry ice slush bath. ^{31}P, ^{19}F, and ^{1}H NMR spectra of the η^1-diphosphetene complexes were recorded at −50 °C.

X-ray Crystallographic Determination of the Structure of 9.[15] A

---

(6) Meriem, A.; Majoral, J. P.; Revel, M.; Navech, J. *Tetrahedron Lett.* **1983**, *24*, 1975.

(7) Becker, G.; Becker, W.; Uhl, G. *Z. Anorg. Allg. Chem.* **1984**, *518*, 21.

(8) Appel, R.; Barth, V. *Tetrahedron Lett.* **1980**, *21*, 1923. Appel, R.; Barth, V.; Knoch, F. *Chem. Ber.* **1983**, *116*, 938.

(9) Phillips, I. G.; Cavell, R. G. *Phosphorus Sulfur* **1986**, *30*, 117.

(10) Cowley, A. H.; Hill, K. E. *Inorg. Chem.* **1973**, *12*, 1446.

(11) Shriver, D. F. *The Manipulation of Air-Sensitive Compounds*; Series in Advanced Chemistry: McGraw-Hill: New York, 1969.

(12) Mahler, W.; Burg, A. B. *J. Am. Chem. Soc.* **1958**, *80*, 6161.

(13) Bennett, F. W.; Emeleus, H. J.; Haszeldine, R. N. *J. Chem. Soc.* **1953**, 563.

(14) Collman, J. P.; Hoffman, N. W.; Hosking, J. W. *Inorg. Synth.* **1970**, *12*, 8.

(15) This X-ray crystallographic study comprises Report No. SR:030122-01-86 of the Structure Determination Laboratory, Department of Chemistry, University of Alberta. See paragraph at end of paper regarding supplementary material.

Table II. Crystal Data and Details of Intensity Collection for **9**

A. Crystal Data	
formula	$C_{10}H_{18}F_6P_2Si_2$
fw	370.37
cryst shape	prismatic
cryst dimens	0.22 × 0.38 × 0.37 mm
syst abs	$h + k$ = odd; $h0l$, l odd
space group	monoclinic, $C2/c$ (No. 15)
cell dimens	a = 17.057 (6) Å b = 8.811 (2) Å c = 11.983 (3) Å β = 102.13°
V	1761 Å^3
Z	4
D_{calcd}	1.397 g/cm^3
μ	4.17 cm^{-1}
B. Data Collection and Refinement Conditions	
temp	−65 °C
radiation	Mo Kα (λ = 0.71073 Å)
monochromator	incident beam, graphite cryst
takeoff angle	3.0°
detector aperture	2.40 mm horizontal, 4.00 mm vertical
cryst–detector dist	205 mm
scan type	ω–2θ
scan rate	10.1–1.6°/min
scan width	(0.70 + 0.35 tan θ)°
data colln 2θ limit	54.00°
data colln index range	$h,k,\pm l$
no. of reflcns measd	2038 unique; 1479 with $I > 3\sigma(I)$
observns: variables ratio	1479:91
agreement factors: R_1, R_2, GOF[a]	0.46, 0.57, 2.11

[a] GOF = $[\sum_w(|F_o| - |F_c|)^2/(\text{NO} - \text{NV})^{1/2}]$.

Table III. Positional (×10^4) and Thermal (×10^2) Parameters[a,b] for **9**

atom	x	y	z	U, Å^2
P	648.8 (4)	4058.5 (7)	7481.2 (5)	3.68 (2)[c]
Si	1192.5 (4)	7627.3 (8)	7877.9 (6)	3.32 (2)[c]
F_1	662 (2)	4127 (4)	9750 (3)	7.4 (1)[c]
F_2	1861 (2)	4035 (4)	9357 (3)	7.1 (1)[c]
F_3	1080 (2)	1938 (3)	9103 (3)	6.9 (1)[c]
F_1'	864	2057	9115	11.91[c]
F_2'	1777	3589	9309	6.92[c]
F_3'	715	3990	9817	4.64[c]
C_1	407 (1)	6078 (2)	7617 (2)	2.81 (6)[c]
C_2	900 (2)	9245 (3)	6885 (3)	4.71 (8)[c]
C_3	1350 (2)	8203 (4)	9399 (2)	4.98 (9)[c]
C_4	2133 (2)	6776 (4)	7587 (3)	5.6 (1)[c]
C_5	1047 (2)	3482 (3)	9000 (2)	5.10 (9)[c]

[a] The equivalent isotropic thermal parameter is given by: $U = {}^1/_3(U_{11} + U_{22} + U_{33} + 2U_{23}\cos\alpha + 2U_{13}\cos\beta + 2U_{12}\cos\gamma)$. [b] Those parameters without an esd were not refined. [c] Indicates a value for an atom refined anisotropically.

Table IV. Selected Bond Distances (Å) and Angles (deg)

	Bond Distances[a]		
P–P′	2.223 (1)	F_1–C_5	1.345 (3)
P–C_1	1.841 (2)	F_2–C_5	1.449 (3)
P–C_5	1.874 (2)	F_3–C_5	1.367 (3)
Si–C_1	1.893 (2)	F_1'–C_5	1.308 (2)
Si–C_2	1.857 (2)	F_2'–C_5	1.226 (3)
Si–C_3	1.857 (2)	F_3'–C_5	1.309 (2)
Si–C_4	1.868 (2)	C_1–C_1'	1.356 (3)
	Bond Angles[a]		
P′–P–C_1	75.84 (6)	P–C_5–F_2	109.0 (2)
P′–P–C_5	98.02 (8)	P–C_5–F_3	111.0 (2)
C_1–P–C_5	102.60 (8)	P–C_5–F_1'	108.5 (1)
C_1–Si–C_2	111.24 (8)	P–C_5–F_2'	114.2 (2)
C_1–Si–C_3	108.06 (9)	P–C_5–F_3'	120.6 (1)
C_1–Si–C_4	106.6 (1)	F_1–C_5–F_2	103.4 (2)
C_2–Si–C_3	112.5 (1)	F_1–C_5–F_3	112.1 (2)
C_2–Si–C_4	108.4 (1)	F_2–C_5–F_3	106.8 (2)
C_3–Si–C_4	109.9 (1)	F_2–C_5–F_1'	121.8 (2)
P–C_1–Si	123.19 (9)	F_1'–C_5–F_2'	107.6 (1)
P–C_1–C_1'	102.73 (6)	F_1'–C_5–F_3'	95.6 (2)
Si–C_1–C_1'	133.80 (5)	F_2'–C_5–F_3'	108.6 (2)
P–C_5–F_1	114.0 (2)		

[a] Numbers in parentheses are estimated standard deviations in the least significant digits.

crystal of dimensions 0.22 × 0.38 × 0.37 mm, obtained by sublimation as described above, was mounted on an Enraf-Nonius CAD4F automated diffractometer and cooled to −65 °C in a cold air stream. All measurements were made at this temperature by using graphite-monochromatized Mo Kα radiation (λ = 0.71073 Å). Details of the crystal and measurement parameters are given in Table II.

The automatic peak search and reflection indexing program[16] in conjunction with a cell reduction program showed the crystal to be monoclinic with the following systematic absences: $h + k$ odd and $h0l$, l odd. The space group[17] was determined as either $C2/c$ (No. 15) or Cc (No. 9) and was successfully solved in the centric space group. The intensity data were collected by using an ω–2θ scan ($2\theta \leqslant 54°$) with variable scan rates chosen to give $\sigma(I)/I \leqslant 0.03$ within a time limit of 50 s. Thus improved counting statistics were achieved for weak and intense reflections in a minimum time. Extending the scan range to 25% either side of the calculated range gave a peak/background counting time of 2:1. Changes in two standards during the collection time, measured every 60 min of exposure time, were negligible.

The 2107 reflections collected were corrected for Lorentz, polarization, and background effects. After equivalent forms (R factor for averaging, 0.017) were averaged and systematically absent data were rejected, there were 2038 unique reflections of which 1479 having $I > 3\sigma(I)$ were used in the structure solution and refinement.

The structure was solved[18] by using the direct-methods program MULTAN,[19] which gave the P and Si positions. The usual combination of least-squares refinement and difference Fourier synthesis gave the remaining non-hydrogen atom locations. A crystallographic twofold symmetry axis bisects the P–P and C–C bonds of the ring.

The refinement was carried out by using full-matrix least-squares techniques to minimize $\sum w(|F_o| - |F_c|)^2$ where $w = 4F_o^2/\sigma^2(F_o)^2$. The neutral-atom scattering factors were calculated from tabulated analytical expressions.[20] Anomalous dispersion corrections were applied to all non-hydrogen atoms.[21]

The unique CF_3 group has the fluorine atoms disordered among two major sets and one minor set of positions. The minor set, with an occupancy factor of less than 5%, was not included in the final model. The disorder model was constructed with three F atoms of occupancies 0.6 and another three F atoms of occupancies 0.4. The parameters of the second set of F atoms were fixed (one of the F atoms in this set would not converge) while the rest of the molecule was allowed to converge. The H atoms were included at calculated positions (C–H, 0.95 Å, sp^3 geometry) and assigned fixed isotropic thermal parameters 1.2 times those of the attached C atom. Their positional parameters were constrained to those of the attached C atom. The final agreement factors were R_1 = 0.046 and R_2 = 0.057. The highest peak in the final difference Fourier map (0.48 e Å^{-3}) is located near the Si atom and is without chemical significance. There are no close contacts between molecules. The results are given in Tables III–V and supplementary tables.[15]

Results and Discussions

Copyrolysis of substituted acetylenes and the (trifluoromethyl)cyclopolyphosphanes $[(CF_3)P]_{4,5}$ yielded heterocyclopolyphosphanes in varying yields following eq 1. The principal products, the 1,2-diphosphetene and the 1,2,3-triphospholene were obtained in differing proportions. The yields and some properties

---

(16) The diffractometer programs are those supplied by Enraf-Nonius for operating the CAD4F diffractometer with some local modifications and additions.

(17) *International Tables for X-Ray Crystallography*; Kynoch: Birmingham, England, 1969; Vol. I.

(18) The computer programs used in this analysis include the Enraf-Nonius Structure Determination Package by Frenz (Frenz, B. A. *Computing in Crystallography*; Delft University Press: Delft, Holland, 1978; pp 64–71) and several locally written or modified programs.

(19) Main, P.; Lessinger, L.; Woolfson, M. M.; Germain, G.; Declercq, J. P. "MULTAN 11/82. A System of Computer Programs for the Automatic Solution of Crystal Structures from X-Ray Diffraction Data".

(20) *International Tables for X-Ray Crystallography*; Kynoch: Birmingham, England, 1974; Vol. IV, Table 2.2B.

(21) *International Tables for X-Ray Crystallography*; Kynoch: Birmingham, England, 1974; Vol. IV, Table 2.3.1.

Table V. Comparison of Selected Bond Lengths and Angles in Polyphosphane Heterocycles

	bond lengths, Å				bond angles, deg			torsion angle, deg		dihedral angle, deg	struct work ref
		P—C (mean)			∠P—P—C (mean)		∠P—C=C	∠C—P—P—C			
	P—P	endo	exo	C=C	endo	exo	(mean)	endo	exo	∠P—P/C—C[a]	
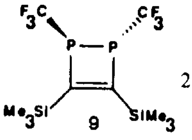 **9**	2.223 (1)	1.841 (2)	1.874 (2)	1.356 (3)	75.84 (6)	98.02 (8)	102.73 (6)	9.68	148.23	12.83[b]	*e*
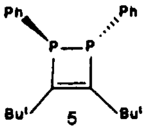 **5**	2.214 (4)	1.847	1.848	1.357 (5)	76.2	103.5	102.8		148.29[c]	19.0[d]	5
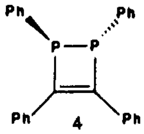 **4**	2.248 (1)	1.830	1.814	1.358 (4)	74.7	107.0	102.1	14	139	10.0[d]	4
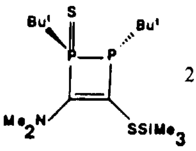	2.219 (1)	1.814	1.873	1.360 (5)	76.25	107.4	103.6				7
$[CF_3P]_4$	2.213 (5)		1.867 (14)			97.8			131.6		25
$[CF_3P]_5$	2.223 (17)		1.906 (20)			101.3 (8)					26

[a] Angle subtended between C=C and P—P vectors. [b] Si—C=C bond angle: 133.80 (5). [c] Calculated from data given in ref 5. [d] C—C=C bond angles: (**5**) 135.9 (3), 134.9 (3)°; (**4**) 131.2 (3)°. [e] This work.

Table VI. NMR Spectroscopic Parameters of 1,2-Diphosphetenes[a]

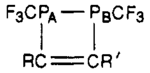

R, R′	compd	$\sigma(P_A)$,[b] ppm	$\sigma(P_B)$,[b] ppm	$\lvert {}^1J_{P_A,P_B} \rvert$, Hz	$\phi(F_A)$,[c] ppm	$\phi(F_B)$,[c] ppm	${}^2J_{F,P}$, Hz	${}^3J_{F,P}$, Hz
CF_3[d]	**1**[f]	−40		55	−54.4		59	18
$SiMe_3$[d,e]	**9**	−31.3		125[d]	−52.2		51.0	8.1
Ph[d,e]	**10**	−54.9		93.8	−55.7		45.4	15.8
CH_3, $Si(CH_3)_3$	**11**	−23.9	−55.5	51.8	−52.0	−52.8	43.6 (F_A) 41.9 (F_B)	15.1 18.1

[a] Recorded for $CDCl_3$ solutions at 25 °C; negative shifts for both ^{19}F and ^{31}P spectra are to low frequency (high field) of standard. [b] Relative to 85% H_3PO_4(aq) at 161.9 MHz. [c] Relative to $CFCl_3$ at 376.5 MHz. [d] ^{31}P and ^{19}F NMR spectra are examples of $X_3AA'X'_3$ spin systems[28] ($X = {}^{19}F$, $A = {}^{31}P$). [e] Coupling constants for spectra of **9** and **10** were determined by iterative calculation using the program NUMARIT.[32] [f] Data for **1** from ref 1. [g] $\lvert J_{P_A,P_B} \rvert$ = 125 Hz was chosen to give the best visual fit between experimental and calculated data for **9**.

are listed in Table I. NMR spectroscopic data for **1** and **9**–**11** are presented in Table VI. The reaction is undoubtedly complex, and the mechanism is not known.

Although a thermally forbidden route, the formation of these species can be *formally* regarded[4] as the coupling of a diphosphene (i.e., a species with a P=P bond) with an acetylene. The structural parameters of the bis(trimethylsilyl)diphosphetene **9** and those previously reported for $(C_6H_5)P(C_6H_5)PC(C_6H_5){=}C(C_6H_5)$ (**4**)[4] and $(C_6H_5)P(C_6H_5)PC(t\text{-}C_4H_9){=}C(t\text{-}C_4H_9)$ (**5**)[5] illustrate the concept.

Crystal and Molecular Structure of $(CF_3)P(CF_3)PC(SiMe_3){=}C(SiMe_3)$ (9). The molecular structure of **9**, Figure 1, consists of a nearly planar four-membered ring with the expected trans orientation of CF_3 substituents across the P–P bond. The metrical details of the structure are given in Tables III–V with additional data in the supplementary material.[15] The puckering of the ring, best described by the relationship between the P—P and C=C vectors, is 12.8°. This value indicates marginally looser "acetylene–diphosphene" binding than for **4** (10°) but stronger binding than in the case of **5** (19°). Despite similar "ring-twist" angles in **4** and **9**, the P–P and endo P–C bond lengths and the exo C–P–P–C torsion angle of **9** are closer in value to those of **5** than those of **4**. This suggests that the electronic effect of substituting a trifluoromethyl group for phenyl combined with a decrease in trans-annular steric repulsions have together given rise to the observed degree of puckering.

A crystallographic twofold symmetry axis bisects the P–P and C–C bonds of **9**. The olefinic bond geometry, though close to planar (the torsional angles $Si\text{–}C_1\text{–}C_1'\text{–}Si'$ and $P\text{–}C_1\text{–}C_1'\text{–}P'$ are 3.39 and 15.80° respectively while the sum of the bond angles around C_1 (C_1') is 359.72 (12)°), is strongly distorted as evidenced by the $P\text{–}C_1\text{–}C_1'$ and $Si\text{–}C_1\text{–}C_1'$ bond angles of 102.7 (6) and 133.80 (5)° respectively. The degree of angular distortion closely parallels that of **4** and **5** (Table V). In particular we note that the silyl methyls of **9** are staggered in a manner nearly identical with that of the *tert*-butyl methyl groups of **5**. In addition one of the silicon carbon bonds, $Si\text{–}C_3$ ($Si'\text{–}C_3'$) is inclined toward the

Table VII. ^{19}F NMR Spectroscopic Parameters of η^1-Diphosphetene Complexes[a]

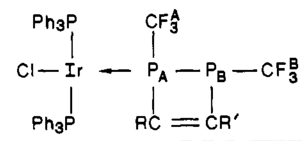

R, R′	compd	$\phi(F_A)$,[b,c] ppm	$^2J_{F_A,P_A}$, Hz	$^3J_{F_A,P_B}$, Hz	$\phi(F_B)$,[b,c] ppm	$^2J_{F_B,P_B}$, Hz	$^3J_{F_B,P_A}$, Hz
CF_3[d]	**12**	−59.9	61.6	23.7	−43.7	42.8	9.9
Ph	**13**	−55.6	50.2	21.7	−42.8	38.1	11.2
CH_3, $Si(CH_3)_3$	**14**	−56.5	43.1	25.8	−43.4	38.6	12.3

[a] Recorded for $CDCl_3$ solutions at −50 °C. [b] Recorded at 376.5 MHz relative to $CFCl_3$; negative shifts are to low frequency (high field) of standard. [c] PCF_3 fluorine resonances are doublets of doublets. [d] CCF_3 fluorine signals at −63.1 and −63.2 ppm, broad singlets.

Table VIII. ^{31}P NMR Parameters of η^1-Diphosphetene Complexes

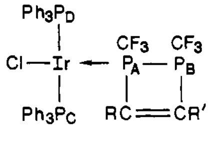

R, R′	compd	$\sigma(P_A)$,[b] ppm	$\sigma(P_B)$,[b] ppm	$^1J_{P_A,P_B}$, Hz	$^2J_{P_A,P_C}$, Hz	$^2J_{P_A,P_D}$, Hz	$\sigma(P_C)$,[d,e] ppm	$\sigma(P_D)$,[d,e] ppm	$^2J_{P_C,P_D}$, Hz
CF_3	**12**	+21.3[b]	−7.0[b]	96.3	25.0	26.1	+25.9	+22.3	341.1
Ph	**13**	+22.2[b]	+1.6[c]	97.1	22.8	24.7	+26.5	+22.9	349.5
CH_3, $SiMe_3$	**14**	+53.9[b]	+14.4[c]	80.7	21.6	26.7	+26.1	+23.1	348.7

[a] Recorded for $CDCl_3$ solutions at −50 °C relative to 85% H_3PO_4(aq) at 161.9 MHz; positive shifts are to high frequency (low field) of the standard. [b] Broad multiplets. [c] Doublet of quartets of quartets. [d] P_C and P_D are labeled arbitrarily. [e] AB spin system.

adjacent phosphorus–CF_3 substituent so as to approximately bisect the F_1–C_5–F_2 (F_1'–C_5'–F_2') bond angle. Thus two methyls on one of the $SiMe_3$ substituents lie on one side of the ring plane diagonally opposite a P–CF_3 group and adjacent to a methyl group of the other $SiMe_3$ group.

Similarly staggered pairs of adjacent Me_3Si substituents are noted in the congested olefin 1,1,2,2-tetrakis(trimethylsilyl)ethene (∠Si—C═C, mean 124.1 (4)°)[22] and in the titanacyclobutene $[(\eta^5\text{-}C_5H_5)_2\overline{TiCH_2C(SiMe_3)=C}(SiMe_3)]$ (∠SiC═C, 130.07–139.62°)[23] though in the former a pronounced twist (29.5°) of the double bond assists in alleviating steric pressure while the asymmetric olefin of the latter is planar. In contrast, steric pressure between the adjacent Me_3Si groups in the essentially trigonal-bipyramidal complex $[Os(CO)_4(\eta^2\text{-}Me_3SiC{\equiv}CSiMe_3)]$ is negligible.[24] The much larger Si—C═C bond angles of the η^2-acetylene (153.0 (8) and 160.0 (8)°) allow the silyl methyl groups to eclipse. In this case the acetylene and two carbonyls that defined the trigonal plane were aligned such that each Os–CO equatorial bond axis eclipsed a Me–Si–Me angle bisector.[24]

The P–P bond length in **9** (2.223 (1) Å) compares favorably with the P–P single bond lengths in $[(CF_3)P]_4$ (2.213 (5) Å)[25] and $[(CF_3)P]_5$[26] (mean 2.223 (17) Å) and lies between the P–P bond lengths in **4** (2.248 (1)[4] Å) and **5** (2.214 (4)[5] Å). Despite a conceivably greater degree of ring strain imposed by the much shorter P–C (endo) and olefinic bond lengths the exo P–P–C bond angle of **4** (98.02 (8)°) is almost identical with that of $[(CF_3)P]_4$ (97.8°).[25] However, the ring strain imposed in approaching planarity is reflected in, and is most probably largely responsible for, the exo C–P–P–C torsional angle in **8** (148.23°) that is markedly more open than that in $[(CF_3)P]_4$ (131.6°),[25] which is folded with a ring-torsion angle (P–P–P–P) of 34°.

Reactions with $[IrCl(N_2)(PPh_3)_2]$. The diphosphetenes **1** and **9–11** react with *trans*-$[IrCl(N_2)(PPh_3)_2]$ in chloroform solution at −50 °C with rapid dinitrogen evolution accompanied by dramatic solution color changes from pale yellow to deep wine red. Except for the case of **9**, new single species were quantitatively produced and were identified by ^{19}F NMR spectra. In particular, the four signals for the product from reaction of **1**, two sets of doublets of doublets and two broad singlets, correspond to two CF_3P and two CF_3C substituents, respectively. The fluorine signals observed previously for the complex $[Fe(CO)_4\{\overline{(CF_3)P(CF_3)P\text{-}C(CF_3)=C}(CF_3)\}]$[10] (**6**) are similar in character to those observed for our Ir η^1 complexes. In all cases the similar asymmetric $(PCF_3)_2$ moieties that are observed in ^{19}F NMR spectra of the reaction products (Table VII) indicate that the diphosphetene ligands are bound to the metal by coordination of a single phosphorus lone pair. We therefore suggest that dinitrogen is associatively displaced from *trans*-$[IrCl(N_2)(PPh_3)_2]$ by **1**, **10**, and **11** without either loss of configuration at the metal *or* ring cleavage (eq 3).

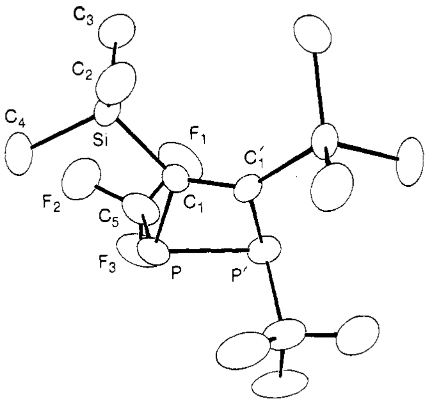

Figure 1. ORTEP perspective view of a molecule of $\overline{(CF_3)P(CF_3)PC\text{-}(SiMe_3)=C}(SiMe_3)$ (**9**) showing the atom-numbering scheme. The atoms are represented by thermal ellipsoids at the 50% probability level. H atoms have been omitted for clarity as have the F atoms of the disordered model. The primed atoms are related to the unprimed atoms by a crystallographic twofold axis.

This formulation is supported by the ^{31}P NMR spectra (Table VIII). In **12**, **13**, and **14** the Ph_3P phosphorus nuclei resonate as AB spin systems characterized by large $J_{A,B}$ values of 340–350

---

(22) Sakurai, H.; Nakadaira, Y.; Tobita, H.; Ito, K.; Toriumi, K.; Ito, H. *J. Am. Chem. Soc.* **1982**, *104*, 300.

(23) McKinney, R. J.; Tulip, D. H.; Thorn, D. L.; Coolbaugh, T. S.; Tebbe, F. N. *J. Am. Chem. Soc.* **1981**, *103*, 5584.

(24) Ball, R. G.; Burke, M. R.; Takats, J. *Organometallics* **1987**, *6*, 1918.

(25) Palenik, G. J.; Donahue, J. *Acta Crystallogr.* **1962**, *15*, 564.

(26) Spencer, C. J.; Lipscomb, W. N. *Acta Crystallogr.* **1961**, *14*, 250.

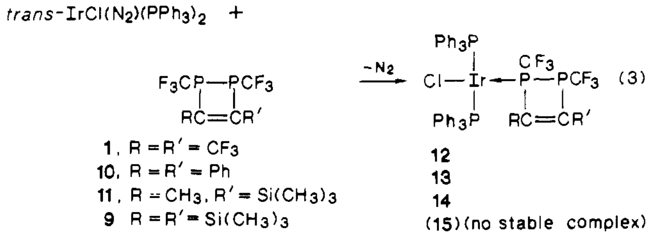

1, R = R' = CF_3 — 12

10, R = R' = Ph — 13

11, R = CH_3, R' = $Si(CH_3)_3$ — 14

9 R = R' = $Si(CH_3)_3$ — (15) (no stable complex)

Hz, which are typical[27] of ${}^2J_{P,P}$ for *trans*-disposed tertiary phosphanes in square-planar or octahedrally coordinated transition-metal compounds. The observed inequivalence of the triphenylphosphanes and the pattern in the ^{31}P NMR spectra even at +25 °C for **14** are consistent with asymmetry introduced by restricted rotation of the η^1-coordinated diphosphetene. In addition each of the phosphorus atoms of the Ph_3P groups is independently split by coupling to one other nucleus of spin = $^1/_2$. The magnitudes of these splittings (21.6–26.7 Hz) are characteristic of ${}^2J_{P,P}$ between cis-disposed tertiary phosphorus nuclei. As a result we place the triphenylphosphane ligands cis to the unique coordinating phosphorus atom of the ring and trans to each other.

Finally, the shifts of the coordinated ring phosphorus nuclei are found from 54 to 78 ppm to low field of the shifts in the free rings. In **12**–**14** the uncoordinated ring phosphorus nuclei also show substantial changes in chemical shift to lower field relative to the resonances of the same atoms in the free rings, but of consistently smaller magnitude.

Selective ^1H-decoupled ^{31}P and ^{31}P-decoupled ^1H NMR spectra of **14** confirm that it is solely the phosphorus nucleus that is coupled to, and hence adjacent to, the methyl group on the carbon backbone that coordinates to iridium. We think that the lesser steric bulk of the methyl as compared to the trimethylsilyl substituent is the dominant factor governing the product distribution although the different basicities of the two phosphorus atoms could also be important.

When we consider that *trans*-$[IrCl(N_2)(PPh_3)_2]$ is very stable in chloroform solution below 0 °C, compound **9** has clearly demonstrated its ability to displace dinitrogen from the metal substrate at −50 °C, presumably by an associative displacement mechanism. We propose that steric crowding within the expected product (**15**, R = R' = $SiMe_3$, eq 3) makes the complex thermally unstable with respect to ligand dissociation even at −50 °C and allows the resultant $[IrCl(PPh_3)_2]$ moiety to decompose by pathways normally only available to it at higher temperatures. ^{31}P and ^{19}F NMR spectra of reaction mixtures show largely free **9** and various unidentified Ir–PPh_3 species which are however virtually identical with those obtained from decomposition of $[IrCl(N_2)(PPh_3)_2]$ at higher temperatures in chloroform.

All three η^1-diphosphetene complexes are stable indefinitely when stored at −78 °C, but at +25 °C, significant further reaction occurs. Compound **14** slowly releases ring **11** over 2 days at +25 °C, and the resultant products are identical with the decomposition products obtained from the reaction of *trans*-$[IrCl(N_2)(PPh_3)_2]$ and **9** at −50 °C. Partial decomposition (ca. 40%) of **13** by ring dissociation occurs within 3 h at +25 °C to give a product mixture that, except for a new species, **17**, which accounts for 60% of the total fluorine NMR intensity, is also identical with that obtained from the reaction of ring **9**. Reaction mixtures containing **17** are dark blue. Compound **12** transforms quantitatively to a new single species, **16**, whose ^{19}F and ^{31}P NMR characteristics clearly indicate that it is of the same family of complexes as **17** (Table IX). Compound **16**, like **12**, is dark wine red.

The $^{31}P\{^1H\}$ NMR spectra of **16** and **17** each show two phosphorus resonances of equal intensity: a broad multiplet (+76.8 and +59.0 ppm, respectively) and a sharp 1:2:1 triplet (+5.9 and +9.3 ppm with splittings of 19.0 and 23.5 Hz, respectively). The high-field triplet signals demonstrate that the Ph_3P substituents are now equivalent and are symmetrically coupled to two mutually cis phosphorus nuclei.

Table IX. ^{31}P and ^{19}F NMR Parameters of Metallacyclic Compounds[a]

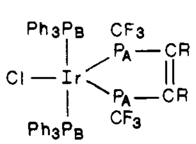

R	compd	$\sigma(P_A)$,[b,d] ppm	$\sigma(P_B)$,[b,e] ppm	${}^2J_{P_A,P_B}$, Hz	$\phi(F)$,[c,f] ppm	$\lvert {}^2J_{P_A,F} + {}^4J_{P_A,F}\rvert$, Hz
CF_3	**16**[g]	+76.8	+5.9	19.0	−49.6	63.4
Ph	**17**	+79.3	+9.3	23.5	−47.3	54.6

[a] Recorded in $CDCl_3$ solution at +25 °C. [b] Relative to 85% H_3PO_4; positive shifts are to high frequency (low field) of standard at 161.9 MHz. [c] Relative to $CFCl_3$; negative shifts are to low frequency of (high field) standard at 376.5 MHz. [d] P_A resonances are multiplets that collapse to 1:2:1 triplets with ^{19}F decoupling. [e] P_B resonances are 1:2:1 triplets. [f] CF_3 resonances are X parts of $X_3AA'X'_3$ spin systems. Estimates[28] of $\lvert {}^2J_{P_A,P_B}\rvert$: 45 Hz (**16**) and 43 Hz (**17**). [g] CCF_3 resonance $\phi(F)$: −57.9 ppm, a complex multiplet.

In $^{31}P\{^{19}F\}$ NMR spectra of **17**, the low-field broad multiplet collapses to a 1:2:1 triplet with a splitting of 23.5 Hz. The Ph_3*P* and CF_3*P* phosphorus signals represent both halves of an A_2X_2 spin system. The fluorine resonance patterns of the CF_3P portions of **16** and **17** are typical of $X_3AA'X'_3$ spin systems (the X part) where $J_{X,X'}$ is zero.[28] From fluorine spectra $\lvert J_{P,P}\rvert$ estimates of 45 and 43 Hz, respectively, are obtained. The former is 10 Hz lower in magnitude than $\lvert {}^1J_{P,P}\rvert$ for ring **1**.

The most reasonable interpretation of the ^{19}F and ^{31}P NMR spectroscopic patterns is that the diphosphane moiety of rings **1** and **10** have participated in [3 + 2] addition reactions across the metal (eq 4). The ring phosphorus atoms of **17** are magnetically equivalent when fluorine decoupled (half of an A_2X_2 spin system) but inequivalent when coupled (the A part of an $X_3AA'X'_3$ spin system[28]).

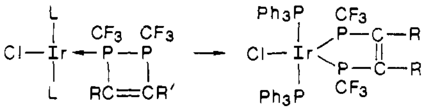

12, R=R'=CF_3 — 16, R = R' = CF_3

13, R=R'=Ph — 17, R = R' = Ph

These NMR data strongly suggest that C_2 symmetry is preserved about the Ir–Cl axis. Clearly the triphenylphosphanes are perpendicular (i.e., trans) to this axis. If the metallacycle ring is rigid, either the chloride, the ring atoms, and the CF_3 carbons are coplanar with the metal or the ring and CF_3 carbons are twisted in such a fashion as to preserve a C_2 symmetry axis through the centroid of the metallacyclic ring and Cl. This latter alternative preserves at least some pyramidal character at phosphorus. An additional possibility is that the rings are puckered with a transoid distribution of phosphorus–CF_3 substituents that equilibrate rapidly by a bond-rotation–ring-puckering mechanism:

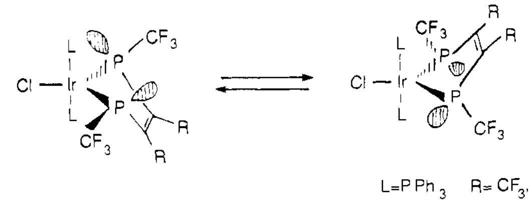

L=PPh3 R= CF3, Ph

In this latter case an exchange process rapid on the NMR time scale is required to render both Ph_3P nuclei equivalent. We have however observed no changes in ^{19}F or ^{31}P NMR spectra between −50 and +25 °C, indicating that this explanation of the observed spectral pattern is unlikely.

A similar fluxional process is known to operate for titanocene–alkenedithiolate complexes[29,30] and related selenium ana-

---

(27) Nixon, J. F.; Pidcock, A. *Annu. Rev. NMR Spectrosc.* **1969**, *2*, 345.

(28) Harris, R. K. *Can. J. Chem.* **1964**, *42*, 2275.

Inorg. Chem. 1988, 27, 2275–2278

logues[30] where inversion of configuration of the main-group element effects site exchange. Barriers to site exchange in these cases ($\Delta G^{\ddagger}$, 14.3–17.8 kcal mol^{-1}) are comparble to the lowest energy barriers measured for inversion of configuration of phosphane phosphorus nuclei with two organic and one transition-metal complex substituent. Gladysz et al.[31] have shown that barriers to inversion at phosphide phosphorus bound to Ru lie in the range 11–14 kcal. The exchange process to be invoked above would therefore necessarily require an unprecedented low barrier to inversion in order that such a process be the source of the observed spectral patterns and their temperature independence. Although we cannot rule out such a facile exchange process, we think, in view of the barriers noted above, that rapid exchange is unlikely.

Conclusions

Although the (trifluoromethyl)diphosphetene ligands described herein are weak bases because of the presence of electron-withdrawing CF_3 substituents on phosphorus, they are sufficiently basic to displace a weakly bound ligand (N_2) from Ir^{I}. The coordination complexes so formed are stable only at reduced temperatures and only if the backbone substituents on carbon are not too bulky. The η^1 coordination complexes are intermediate for the formation of metallacycles by means of an oxidative addition of the P–P bond to Ir^{I}. The resultant Ir^{III} metallacycles appear to be stable only if the backbone carries a substituent with some electron-withdrawing character (e.g., CF_3 or phenyl) perhaps because electron delocalization into the metallacyclic framework is necessary to stabilize the structure.

Acknowledgment. We thank the NSERC (Ottawa) for financial support.

Registry No. **1**, 114297-14-2; **9**, 114198-79-7; **10**, 114198-80-0; **11**, 114220-87-0; **11b**, 114198-81-1; **12**, 114198-75-3; **13**, 114198-76-4; **14**, 114198-77-5; **16**, 114198-78-6; **17**, 114220-86-9; $[(CF_3)P]_4$, 393-02-2; $[(CF_3)P]_5$, 745-23-3; $Me_3SiC{\equiv}CSiMe_3$, 14630-40-1; $PhC{\equiv}CPh$, 501-65-5; $MeC{\equiv}CSiMe_3$, 6224-91-5; $[IrCl(N_2)(PPh_3)_2]$, 15695-36-0.

Supplementary Material Available: Anisotropic thermal parameters (Table X), derived positional and thermal parameters for hydrogen atoms (Table XI), RMS amplitudes of thermal vibration (Table XII), all bond angles (Table XIII), and torsional angles (Table XIV) (4 pages); calculated and observed structure factors (Table XV) (10 pages). Ordering information is given on any current masthead page.

---

[29] Kopf, H. *Angew. Chem., Int. Ed. Engl.* **1971**, *10*, 134.
[30] Bolinger, C. M.; Rauchfuss, T. B. *Inorg. Chem.* **1982**, *21*, 3947.
[31] Buhro, W. E.; Gladysz, J. A. *Inorg. Chem.* **1985**, *24*, 3507.
[32] J. S. Martin, University of Alberta, and K. Worvill, University of East Anglia; personal communication from J.S.M.

Contribution from the Department of Chemistry,
University of California, Davis, California 95616

Metallamacrocycles Built from Mercury(II) and Bis((diphenylphosphino)methyl)phenylarsine

Alan L. Balch,* Marilyn M. Olmstead, and Steven P. Rowley

Received December 8, 1987

Addition of bis((diphenylphosphino)methyl)phenylarsine (dpma) to $[Hg\{(CH_3)_2SO\}_6][O_3SCF_3]_2$ in methanol followed by the addition of ammonium hexafluorophosphate yields $[Hg_2(\mu\text{-dpma})_2(O_3SCF_3)_2(CH_3OH)_3][PF_6]_2{\cdot}CH_3OH$ (**3**). Colorless parallelepipeds of this crystallize in the in the triclinic space group $P\bar{1}$ (No. 2) with a = 12.273 (4) Å, b = 16.941 (5) Å, c = 20.468 (5) Å, α = 93.77 (2)°, β = 91.70 (2)°, and γ = 105.47 (2)° at 130 K. Least-squares refinement of 600 parameters using 8139 reflections yielded R = 0.069, R_w = 0.074. The structure consists of a $Hg_2(dpma)_2$ metallamacrocycle with nearly linear P–Hg–P coordination. One trifluoromethanesulfonate bridges the two mercury ions. One mercury is loosely coordinated by two methanol molecules, while the other is bound to one methanol and one monodentate trifluoromethanesulfonate. Treatment of **3** with tin(II) chloride yields $[Hg_2(\mu\text{-dpma})_2(\mu\text{-Cl})_2][PF_6]_2$ (**4**). Colorless parallelepipeds of **4** belong to the triclinic space group $P\bar{1}$ (No. 2) with a = 10.351 (3) Å, b = 13.514 (5) Å, c = 14.297 (5) Å, α = 62.95 (2)°, β = 77.78 (2)°, and γ = 70.73 (2)° at 130 K. Least-squares refinement of 207 parameters using 5275 reflections yielded R = 0.037, R_w = 0.042. The structure of the centrosymmetric dication involves a $Hg_2(dpma)_2$ metallamacrocycle with two bridging chloride ligands. Each mercury has grossly distorted tetrahedral geometry. Comparison of the structures of **3** and **4** indicates the $Hg_2(dpma)_2{}^{4+}$ metallacycle must fragment into $Hg_2(dpma)^{4+}$ and dpma units or into two $Hg(dpma)^{2+}$ units during the conversion of **3** into **4**.

Introduction

The metallamacrocycles **1** and **2**, which involve two planar, d^8 metal ions, have been shown to bind a variety of cations, anions, and neutral molecules.[1-11] The combination of traditional Lewis base binding sites (N or As) and the amphoteric d^8 metal ions gives these macrocycles a unique ability to interact with substrates.

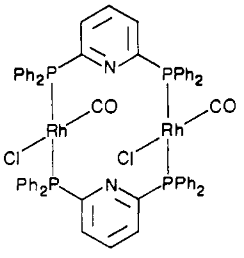

1

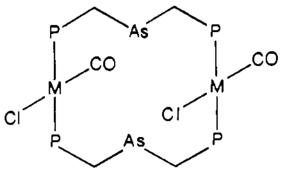

2

In order to expand the range of such metallamacrocycles, we have undertaken the preparation of new examples involving different

---

* Address correspondence to this author.

[1] Balch, A. L. *Pure Appl. Chem.* **1988**, *60*, 555.
[2] Wood, F. E.; Hvoslef, J.; Balch, A. L. *J. Am. Chem. Soc.* **1983**, *105*, 6986.
[3] Wood, F. E.; Hvoslef, J.; Hope, H.; Balch, A. L. *Inorg. Chem.* **1984**, *23*, 4309.
[4] Balch, A. L.; Hope, H.; Wood, F. E. *J. Am. Chem. Soc.* **1985**, *107*, 6936.
[5] Balch, A. L.; Fossett, L. A.; Olmstead, M. M.; Oram, D. E.; Reedy, P. E., Jr. *J. Am. Chem. Soc.* **1985**, *107*, 5272.
[6] Balch, A. L.; Fossett, L. A.; Guimerans, R. R.; Olmstead, M. M.; Reedy, P. E., Jr. *Inorg. Chem.* **1986**, *25*, 1397.
[7] Balch, A. L.; Fossett, L. A.; Olmstead, M. M.; Reedy, P. E., Jr. *Organometallics* **1986**, *5*, 1929.
[8] Balch, A. L.; Ghedini, M.; Oram, D. E.; Reedy, P. E., Jr. *Inorg. Chem.* **1987**, *26*, 1223.
[9] Balch, A. L.; Oram, D. E.; Reedy, P. E., Jr. *Inorg. Chem.* **1987**, *26*, 1836.
[10] Balch, A. L.; Nagle, J. K.; Olmstead, M. M.; Reedy, P. E., Jr. *J. Am. Chem. Soc.* **1987**, *109*, 4123.
[11] Bailey, D. A.; Balch, A. L.; Fossett, L. A.; Olmstead, M. M.; Reedy, P. E., Jr. *Inorg. Chem.* **1987**, *26*, 2413.

0020-1669/88/1327-2275$01.50/0 © 1988 American Chemical Society